

# RSC Advances



This is an *Accepted Manuscript*, which has been through the Royal Society of Chemistry peer review process and has been accepted for publication.

*Accepted Manuscripts* are published online shortly after acceptance, before technical editing, formatting and proof reading. Using this free service, authors can make their results available to the community, in citable form, before we publish the edited article. This *Accepted Manuscript* will be replaced by the edited, formatted and paginated article as soon as this is available.

You can find more information about *Accepted Manuscripts* in the [Information for Authors](#).

Please note that technical editing may introduce minor changes to the text and/or graphics, which may alter content. The journal's standard [Terms & Conditions](#) and the [Ethical guidelines](#) still apply. In no event shall the Royal Society of Chemistry be held responsible for any errors or omissions in this *Accepted Manuscript* or any consequences arising from the use of any information it contains.

# Revealing the thermal sensitivity of lignin during glycerol thermal processing through structural analysis

Wei Zhang<sup>a</sup>, Noppadon Sathitsuksanoh<sup>bc</sup>, Blake A. Simmons<sup>cd</sup>, Charles E. Frazier<sup>a</sup>, Justin Barone<sup>e</sup>, and Scott Renneckar<sup>\*af</sup>

<sup>a</sup> Macromolecules and Interfaces Institute and Department of Sustainable Biomaterials, Virginia Polytechnic Institute and State University, Blacksburg, VA, 24061, United States

<sup>b</sup> Department of Chemical Engineering and Conn Center for Renewable Energy Research, University of Louisville, Louisville, Kentucky 40292, USA

<sup>c</sup> Deconstruction Division, Joint BioEnergy Institute, Lawrence Berkeley National Laboratory, Emeryville, CA, 94608

<sup>d</sup> Biological and Engineering Sciences Center, Sandia National Laboratories, Livermore, CA, 94551

<sup>e</sup> Macromolecules and Interfaces Institute and Department of Biological Systems Engineering, Virginia Polytechnic Institute and State University, Blacksburg, 24061, United States

<sup>f</sup> Department of Wood Science, University of British Columbia, Forest Sciences Centre 4034, 2424 Main Mall, Vancouver, British Columbia V6T 1Z4, Canada. E-mail: scott.renneckar@ubc.ca; Tel: 604-827-0637

† Electronic supplementary information (ESI) available.

**Keywords** lignin isolation, pretreatment, glycerol thermal processing, structural analysis

**Abstract** Woody biomass was treated in glycerol between 200 and 240 °C in an anhydrous environment to denature biomass for biopolymer fractionation. After glycerol thermal processing (GTP), up to 41% of the initial Klason lignin of the starting biomass was recovered in a powdered form through a room temperature dioxane extraction followed by precipitation. <sup>31</sup>P-nuclear magnetic resonance (NMR) of the GTP lignin revealed the syringyl phenolic functionality increased linearly with the log of the severity parameter establishing the impact of the thermal processing on structure. Further structural analysis via thioacidolysis and two-dimensional (2D) <sup>13</sup>C-<sup>1</sup>H heteronuclear single quantum coherence (HSQC) NMR of the isolated lignin indicated GTP caused extensive β-O-4 bond decomposition and the liberated phenolic OH did not undergo further coupling. At the same time, condensation occurred on the aromatic C<sub>5</sub> position of the phenylpropane units to yield GTP lignin with a relatively high molecular weight, comparable to that of enzymatic mild acidolysis lignin from non-thermally treated fibers. The recovered GTP lignin was more thermally stable compared to nearly all other lignin found in the literature. Additionally, the glass transition temperature was invariant to processing severity parameters. These structural changes indicate lignin is highly sensitive to moderately high temperatures common to thermoplastic polymer processing conditions.

## Introduction

Lignin is one of the most abundant biopolymers on earth, but also one of the most perplexing to convert into an industrial feedstock for polymeric applications. The paper-making industry is the

major source of isolated lignin derived from sulfite and sulfate pulp production. The resulting lignin is partially depolymerized and recondensed into fractions that are commonly used as a heating resource in paper mills.<sup>1,2</sup> Furthermore, there is a strong specialties market for selected lignin polymers<sup>1,3,4</sup> such as lignosulfonates, due to their self-assembling properties.<sup>5</sup> However, the most abundant form of isolated lignin, kraft lignin, has not breached the commercial market as a renewable replacement for many thermoplastic applications, although the thermal properties can be tailored by substitution.<sup>6</sup> Recently, the thermal stability of kraft lignin was analyzed revealing a dramatic increase in molecular weight as function of heating time.<sup>7</sup> The study showcased the issues of utilizing kraft lignin without further derivitization to limit degradation reactions when exposed to elevated temperatures.<sup>7</sup> Moreover, other pilot scale lignins such as steam-exploded lignin and organosolv lignin have shown enhanced performance relative to kraft lignins when used in polymeric applications.<sup>1,8-10</sup> Hence, the rearrangement of lignin structure during pulping operations can negatively impact the utilization of lignin placing them in a transitory state that can change during further thermal processing, high temperature solvent derivatization, or even during analysis. Therefore, new methods to control functionality during isolation should be carefully viewed as a means to enhance the qualification of lignin for polymeric applications.

The nascent biorefinery industry pretreats biomass to unlock the recalcitrant structure of lignocellulose and this process involves thermal energy in some form. The pretreatment processes render carbohydrates more accessible to enzymatic saccharification and fermentation, and at the same time, allow lignin separation for further utilization as a co-product. Unlike traditional pulping, fiber quality is not important, so new delignification methods to access the polysaccharides are not limited by the impact they have on paper properties. There are several

pretreatment methods that were developed to reach efficient separation of carbohydrates and lignin, including dilute acid exposure, alkali soaks, steam explosion processing, hydrothermal treatments, organosolv pulping, ionic liquids treatment, as well as mechanical and biological methods.<sup>11, 12</sup> Lignin isolated from steam-exploded or hydrothermal treated biomass is more heterogeneous because of the simultaneous depolymerization<sup>13, 14</sup> and repolymerization.<sup>13, 15</sup> Acid pretreatment<sup>11</sup> not only results in severe lignin degradation and condensation but also can cause equipment corrosion. In contrast, organosolv pretreatment is a potential candidate to produce high quality lignin with low molecular weight and high purity,<sup>1, 16</sup> which has been utilized to develop lignin based bioplastics. The most common solvents used in organosolv pretreatment are aqueous ethanol or acetone liquors combined with an acid catalyst based on the “Alcell” process.<sup>17</sup>

Additionally, other organic solvents such as glycols have been used in the pretreatment of biomass. Studies using aqueous glycerol with alkaline catalysts resulted in direct lignin removal causing lignin degradation into low molecular weight fragments.<sup>18-20</sup> Different from the alkaline catalyzed glycerol pretreatment, researchers at the University of Sherbrook in the 1980’s built a demonstration scale processing unit to treat wood flour up to 20% mass in ethylene glycol.<sup>21</sup> The samples were transferred through a high shearing reciprocating valve assembly and then heated to 220 °C. The authors reported that solvolysis took place where the solvent caused disruption of the wood components making the lignin extractable directly into ethylene glycol in good yields.

Recently another approach for biomass pretreatment was studied involving anhydrous glycerol, based on its ability to serve as a plasticizing agent for melt-processed biopolymers and protecting them from thermal degradation.<sup>22</sup> As such, woody biomass was mixed and sheared with glycerol at high temperature, without acid or alkali catalysts, to denature woody biomass

structure in order to fractionate the biopolymers.<sup>23</sup> The processing served as a pretreatment in order to enhance the digestibility of the cellulose in the fiber.<sup>24</sup> Furthermore, the process was significantly different from past attempts in glycerol pulping, as it did not extract the lignin directly into the liquor. After this glycerol thermal processing, polymeric lignin was simply extracted from the fiber as a co-product. The following study builds from this initial study, analyzing the structure and functionality of the recovered lignin after glycerol thermal processing of woody biomass. The processing of biomass under these conditions provided a path towards a unique lignin structure that has several novel characteristics and additional insight that, although lignin is usually deemed as thermally stable, linkages are extensively cleaved at these moderately high temperatures. These processing temperatures coincide with many thermoplastic melts and provide evidence that activities such as melt processing in benign environments can have a profound impact on lignin structure.

## Results and Discussion

### GTP lignin yield through mild solvent extraction

Aqueous glycerol was demonstrated to swell the wood cell wall and improve solvent penetration.<sup>18, 25</sup> However, glycerol alone only swells wood up to 0.7% (volumetric) at room temperature, but 23% with irreversible change in swelling after heating above the glass transition ( $T_g$ ).<sup>26</sup> In this research, glycerol was introduced at temperatures well above the glass transition of wood providing the ability to swell the wood cell wall under the influence of continuous imposed shear. This process resulted in the disruption of the native cell wall network by the removal of the hemicellulose side chain components such as arabinose and galactose<sup>23</sup> during GTP processing and subsequent water extraction. After pretreatment and water washing, 84% to 92% of total initial Klason lignin, dependent upon GTP severity, was preserved in the biomass. The

subsequent mild solvent extraction without additional catalysts was conducted to isolate lignin from water extracted GTP biomass, with the goal of directly revealing the GTP effects on lignin structure. Note, no lignin could be extracted using aqueous dioxane from non-pretreated sweetgum, so EMAL was used as a control lignin.

Room temperature solvent extraction using aqueous dioxane increased the delignification from 4% to 52% relative to the initial lignin mass as a function of severity parameter. After extraction, the isolated lignin was precipitated with dilute acid and recovered as GTP lignin in a dry powder form. With increased GTP pretreatment severity, the amount of recovered GTP lignin increased linearly with the log of the severity parameter ( $R^2=0.987$ ) (Fig. 1). A maximum of 41% of initial lignin was successfully precipitated and recovered from GTP. The difference between delignification and GTP lignin yield was approximately 10%, which most likely represented the low molecular weight degraded lignin fragments that were non-recoverable from the solvent. In comparison to other studies in the literature, 80% to 90% degraded lignin was solubilized with alkaline aqueous glycerol after long treatment times.<sup>19</sup> For ethylene glycol pulping, 72% of the initial lignin was precipitated under optimized conditions.<sup>27</sup> It is clear that the GTP pretreatment helps to break the connection between lignin and carbohydrate, but does not fully degrade it into non-recoverable fragments.

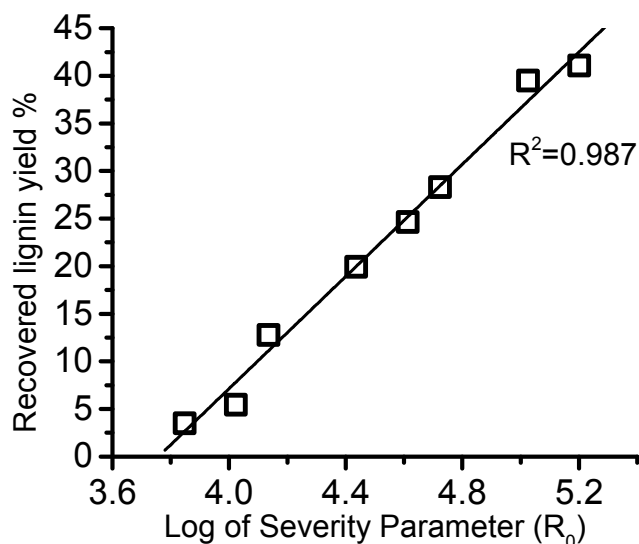


**Fig. 1** Recovered polymeric lignin yield during solvent extraction (average of duplicates with COV<5%) based on processing condition time and temperature, combined into a single severity parameter  $R_0$ . Note mass is based on lignin content in the pretreated fiber.

#### Quantitative $^{31}\text{P}$ -NMR of recovered lignin

Quantitative  $^{31}\text{P}$  NMR<sup>28, 29</sup> was utilized to calculate the contents of aliphatic, phenolic hydroxyl, and carboxylic acid groups in the recovered GTP lignin (Fig. 2a). Total free phenolic OH increased from 0.93 mmol/g lignin in the EMAL that served as a control to 2.33 mmol/g lignin in GTP lignin after the highest severity pretreatment. Previous work showed that alkyl aryl ether bonds were the most vulnerable linkage to be cleaved due to thermolysis,<sup>30</sup> acid catalyzed steam-explosion<sup>13</sup> and organosolv<sup>16, 31</sup> pretreatments creating free phenolics. More importantly, the amount of phenolic OH groups in GTP lignin at the highest severity condition (2.33 mmol/g lignin) was much greater than that in common Alcell and kraft lignins prepared at similar delignification levels (50-60% delignification).<sup>32</sup> In this case, the GTP processing is effective in producing phenolic hydroxyls as functional groups in the isolated lignin.

In contrast, the amount of total aliphatic OH decreased from 5.38 mmol/g lignin for EMAL to 3.39 mmol/g lignin as GTP severity increased (Fig. 2a). This loss of aliphatic OH groups may be



attributed to thermally-induced formaldehyde release through the cleavage of aliphatic OH groups.<sup>30, 33, 34</sup> Jakab et al.<sup>35</sup> reported that formaldehyde release occurred as a result of the thermal scission of  $\gamma$ -CH<sub>2</sub>OH at temperatures as low as 200 °C. It was proposed by Kawamoto and Saka<sup>36</sup> that the hydrogen bonds formed between  $\alpha$ -O and  $\gamma$ -OH in lignin model compounds would ionize the  $\gamma$ -O, further facilitating the C- $\gamma$  elimination with release of formaldehyde. Similar to this mechanism, abundant hydroxyl groups from glycerol during GTP treatment may serve as a source of hydrogen abstraction and form hydrogen bonds with lignin  $\gamma$ -OH in a similar way with the  $\gamma$ -elimination leading to the phenolic vinyl ether intermediates.<sup>37</sup> Clear from these results is the sensitivity of the native structure to thermal processing.

The lignin C<sub>9</sub> formula was determined using elemental analysis and proton NMR (Supporting information Table S1) and used to convert the functional group concentration into numbers per phenylpropane C<sub>9</sub> unit. The number of aliphatic OH in EMAL was 120 units/100C<sub>9</sub>, but in the isolated lignin after GTP pretreatment that number decreased from 97 units/100C<sub>9</sub> to 68 units/100C<sub>9</sub> respectively when log(R<sub>0</sub>) increased from 4.14 to 5.20. The reduced aliphatic hydroxyl content relative to EMAL suggested limited glycerol contamination with free hydroxyls by grafting onto lignin during processing. It was interesting to note at low severity conditions there was first a slight increase in aliphatic hydroxyl content (Fig. 2a) prior to a consistent reduction in aliphatic hydroxyl content.

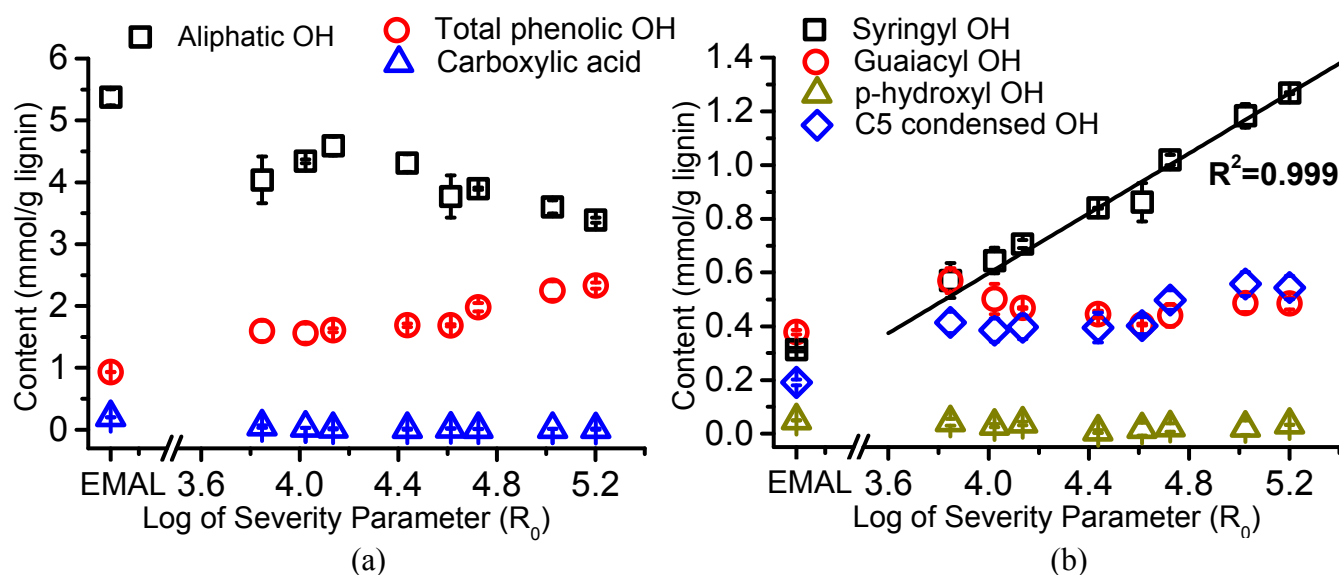


**Fig. 2**  $^{31}\text{P}$  NMR functional group analysis of isolated lignin. (a) Content of aliphatic OH, phenolic OH and carboxylic acid in recovered lignin as a function of the severity parameter  $\log(R_0)$ ; (b) Detailed phenolic OH content in recovered lignin as a function of  $\log(R_0)$ .

Additionally, minimal carboxylic acid amounts in the GTP lignin (0.17-0.35 unit/100C<sub>9</sub>) were observed in Fig. 2a, indicating limited lignin oxidation occurred during the high temperature GTP pretreatment. Argyropoulos et al.<sup>38</sup> reported that EMAL was a useful model for nonoxidized lignin with low carboxylic acid content. In our research, the recovered GTP lignin had even a less degree of oxidization than EMAL.

Quantitative  $^{31}\text{P}$ -NMR spectroscopy with phosphitylation reagent II was reported to resolve various phenolic structures, especially in separating syringyl and C<sub>5</sub>-condensed OH groups.<sup>39</sup> Fig. 2b showed the amount for different phenolic hydroxyls in recovered GTP lignin. The most extraordinary change was observed for syringyl OH, which increased linearly as a function of GTP severity from 0.31 mmol/g lignin (7 units/100C<sub>9</sub>) in EMAL to 1.27 mmol/g lignin (26 units/100C<sub>9</sub>) in GTP lignin at highest severity. In contrast, a small variation between 0.4 and 0.5 mmol/g lignin (8-10 units/100C<sub>9</sub>) in guaiacyl OH content was observed as a function of GTP severity, and p-hydroxyphenyl OH (H) lignin did not change as a function of severity content

after an initial decrease (Fig. 2b). The free phenolic S/G ratio increased from 0.83 for EMAL to 2.6 for GTP lignin, and similar results were reported for aspen lignin after steam-explosion pretreatment.<sup>39, 40</sup> These results indicate that the syringyl phenolic OH was the major product released from alkyl aryl ether bond breakage during the GTP processing. The linear relationship between GTP lignin extraction and syringyl OH yield (Fig. 3) shows that liberating these syringyl phenolics is correlated to the ability to access and remove lignin from the cell wall.

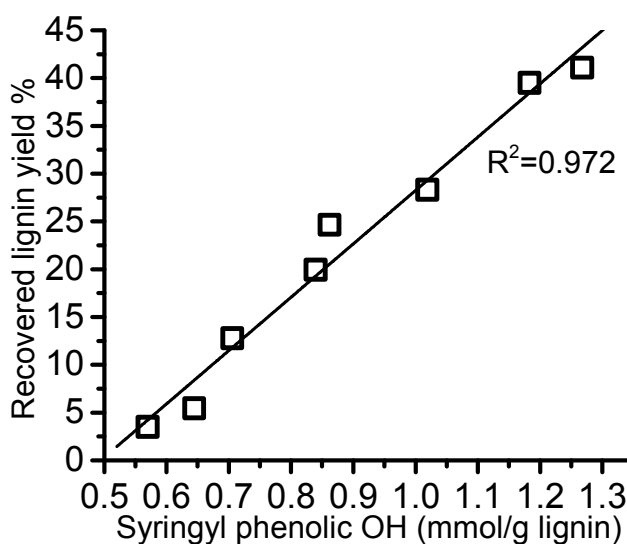


**Fig. 3** Content of syringyl phenolic OH as a function of recovered lignin yield.

C<sub>5</sub> condensed phenolic structures are the phenolic rings with C-C bonds at the C<sub>5</sub> position, such as biphenolic units and diaryl methanes.<sup>28, 39</sup> These structures can be derived from the condensation of the benzylic carbon or guaiacyl and p-hydroxyphenyl units with the free C<sub>5</sub> position under acid or alkaline delignification conditions.<sup>32</sup> As illustrated by Fig. 2b, the maximum amount of C<sub>5</sub> condensed OH groups in GTP lignin was 0.56 mmol/g lignin, which was 3 times more than that in EMAL. GTP lignin was shown to consistently have more C<sub>5</sub> condensed OH groups than EMAL, indicating that the C<sub>5</sub> condensation occurred during GTP

processing. A previous report also demonstrated that the amount of C<sub>5</sub> condensed OH in kraft and organosolv lignin was in the range of 0.35-0.75 mmol/g lignin at similar delignification degree.<sup>32</sup> Thus, the GTP processing resulted in a similar C<sub>5</sub> phenolic condensation in the recovered lignin. According to Funaoka et al.,<sup>41</sup> a diphenylmethane (DPM) type condensation through C- $\alpha$  and adjacent phenolic nuclei readily occurred when wood was heated over 120 °C. DPM type condensation also occurred in alkaline environments.<sup>42</sup> In the present case, the existence of glycerol as a plasticizer during GTP processing could further accelerate this type of DPM condensation by enhancing the mobility of lignin at higher temperature.

### Thioacidolysis-GC of GTP lignin

To investigate further the relationship of alkyl aryl ether bond breakage as a result of GTP processing severity, thioacidolysis was conducted and the results were shown for 3 severity conditions (log(R<sub>0</sub>) is 4.44, 4.72 and 5.20 - analyzed individually) in Table 1.

**Table 1** Contents of  $\beta$ -O-4 bonded G and S units in GTP lignin and non-pretreated biomass.

log(R <sub>0</sub> )	S (mmol/g lignin)	G (mmol/g lignin)	S/G
SGC	1.2	0.45	2.67
4.44	0.77	0.14	5.50
4.72	0.59	0.13	4.54
5.20	0.31	0.087	3.44

SGC refers to the non-pretreated sweet gum control; precision of thioacidolysis has been confirmed by the SGC samples with COV<5%.

The amounts of  $\beta$ -O-4 linked S and G units in non-pretreated biomass confirmed that S units were predominant in this hardwood species with S/G ratio of 2.67. In GTP lignin isolated after pretreatment, the contents of residual  $\beta$ -O-4 bonded S and G units were observed to dramatically

decrease to a quarter or less of the starting material. These results demonstrated that  $\beta$ -O-4 scission occurred during GTP pretreatment, and with increasing GTP severity more  $\beta$ -O-4 linkages were cleaved by the pretreatment, leaving fewer  $\beta$ -O-4 bonded structures. The S/G ratio changes as a function of the processing severity, and it should be noted that the ratios were for aryl-ether bonded C<sub>9</sub> units. Thioacidolysis does not take into account S and G units with free phenolics and the different analytical methods lead to discrepancies, making the direct comparison of S/G ratios difficult. Results in Table 1 were converted to the number per 100 C<sub>9</sub> rings and compared with the <sup>31</sup>P NMR data (Table 2). Native lignin had 27 units/100C<sub>9</sub> and 9.9 units/100C<sub>9</sub> of  $\beta$ -O-4 bonded S and G units, while there were only 6.3 units/100 C<sub>9</sub> and 1.8 units/100 C<sub>9</sub> S and G units still bonded with the  $\beta$ -O-4 in the GTP lignin at the highest pretreatment severity. Table 2 also showed the free phenolic S/G released during GTP pretreatment as determined by <sup>31</sup>P-NMR analysis. Corresponding to the decreasing number of  $\beta$ -O-4 bonded structures at increased GTP severity, more S and G units were produced with free hydroxyl groups.

**Table 2** Amounts/100C<sub>9</sub> of  $\beta$ -O-4 bonded S/G (thioacidolysis) and free phenolic S/G (<sup>31</sup>P-NMR).

log(R <sub>0</sub> )	Thioacidolysis		<sup>31</sup> P-NMR	
	S	G	S-OH	G-OH
SGC (EMAL)	27	9.9	7	8.4
4.44	16	2.9	18	9.4
4.72	12	2.7	21	9.1
5.2	6.3	1.8	26	9.8

Molecular weight of C<sub>9</sub> units in SGC is assumed to be the same as EMAL; S/G represents the β-O-4 bonded syringyl/guaiacyl units; S/G-OH are the syringyl/guaiacyl units bearing free phenolic OH; numbers are calculated based on the average of duplicates.

A detailed comparison of the difference in β-O-4 bonded structures and their corresponding phenolic structures was used to track the fate of S and G units during GTP processing in Table 3. Compared to the number of β-O-4 bonded S and S-OH units in native lignin, low severity GTP pretreatment (log(R<sub>0</sub>)=4.44) decreased the number of β-O-4 bonded S by 11 units/100C<sub>9</sub>, which was the same number as the increment of S-OH groups. As GTP severity increases, the loss in β-O-4 bonded S was about 1 unit/100C<sub>9</sub> more than the increment in S-OH. These results indicated when the GTP condition was relatively mild (low severities), the released S units bear stable phenolic structures without further reaction. The same comparison for G-units showed there was only ~14% of G released to form G-OH structures even after low severity GTP pretreatment. The G-units released probably underwent condensation reactions through coupling, which was in accordance with the increment of C<sub>5</sub> condensed structures revealed from <sup>31</sup>P-NMR. With increasing GTP severity, the changes in G units were not significant (less than 1 unit per 100 C<sub>9</sub> rings).

**Table 3** Amount changes/100C<sub>9</sub> of β-O-4 bonded S and G (thioacidolysis) and free phenolic S and G (<sup>31</sup>P-NMR) as increasing the GTP severity log(R<sub>0</sub>).

delta log(R <sub>0</sub> )	Thioacidolysis		<sup>31</sup> P-NMR	
	ΔS	ΔG	ΔS-OH	ΔG-OH
SGC to 4.44	-11	-7	+11	+1
4.44 to 4.72	-4	-0.2	+3	-0.3
4.72 to 5.20	-5.7	-0.9	+5	+0.7

(-) refers to decrease in number; (+) refers to increase in number; numbers are calculated based on the average of duplicates.

## 2D HSQC of GTP lignin

2D  $^{13}\text{C}$ - $^1\text{H}$  HSQC NMR was used to observe changes in chemical structure in EMAL and GTP lignin. Common structures in the HSQC spectra were color-coded and assigned in accordance with previously published literature.<sup>43-48</sup> Different lignin inter-units and side-chain linkages were readily distinguished in the aromatic (Fig. 4) and aliphatic regions (Fig. 5).

### Aromatic region ( $\delta_{\text{C}}/\delta_{\text{H}}$ 90-130/5.5-8.0 ppm)

As shown by Fig. 4, only trace amounts of H units were detected in the sweet gum EMAL and its cross peak disappeared in the GTP lignin, which was consistent with the minimum presence of p-hydroxyphenyl units from  $^{31}\text{P}$ -NMR. The calculated ratio of S/G was based on the contour volume for the  $\text{C}_2$  and  $\text{C}_6$  carbons on S and oxidized S rings, as well as the  $\text{C}_2$  carbon on G rings (Table 4). As revealed, the ratio of total S and G units increased after GTP pretreatment, from 3.2 in EMAL to 4.1 at moderate, up to 7.6 at high severity. The S/G ratio for GTP lignin at high severity was strikingly larger than common values for hardwood lignin, which normally fall in the range of 1.5 to 3.3.<sup>43, 49</sup> Detailed examination of the aromatic region for GTP lignin suggested more information about the structure of S-type units. It has been widely reported<sup>43, 44, 48, 50</sup> that the S 2/6 cross peak located in the range of 6.4-7.1 ppm, with a center at 6.7 ppm on  $^1\text{H}$ -dimension, is related to unmodified native lignin present in non-derivatized cell walls. However, the cross peak of S 2/6 in GTP lignin exhibited spread contour volume compared to that in EMAL on the  $^1\text{H}$ -dimension, indicating the heterogeneity between different S-type units. Similar spread contour has also been reported for kraft lignin.<sup>47, 51</sup> Based on the chemical shift behavior observed in NMR analysis, the more shielded protons with high electron density would shift upfield. In this case, the electron density of protons on  $\text{C}_2$  and  $\text{C}_6$  positions on S-type units was supposed to increase, causing the contour of S 2/6 to shift upfield. Combined with the previous

result of occurrence of C<sub>5</sub> condensation due to GTP processing, the condensed aromatic units at the C<sub>5</sub> position, such as diaryl ether, would possess a pseudo-S aromatic structure with high electron density around the C<sub>2/6</sub> protons, which would lead to an enlarged cross peak shifting upfield. Thus, the C<sub>5</sub> condensed structures were likely to be counted as S-type aromatic units in HSQC-NMR, resulting in a much larger S/G ratio than that of non-derivatized hardwood lignin. Further studies need to be conducted on model compounds of highly condensed lignin structures to support this theory. Also noteworthy in this data is the low degree of oxidized S-type units in the lignin (Fig. 4). Typical acidolysis products contain Hibbert ketones at the alpha position and the isolated lignin shows a significant decrease in oxidized lignin relative the mild acidolysis, EMAL, control lignin.

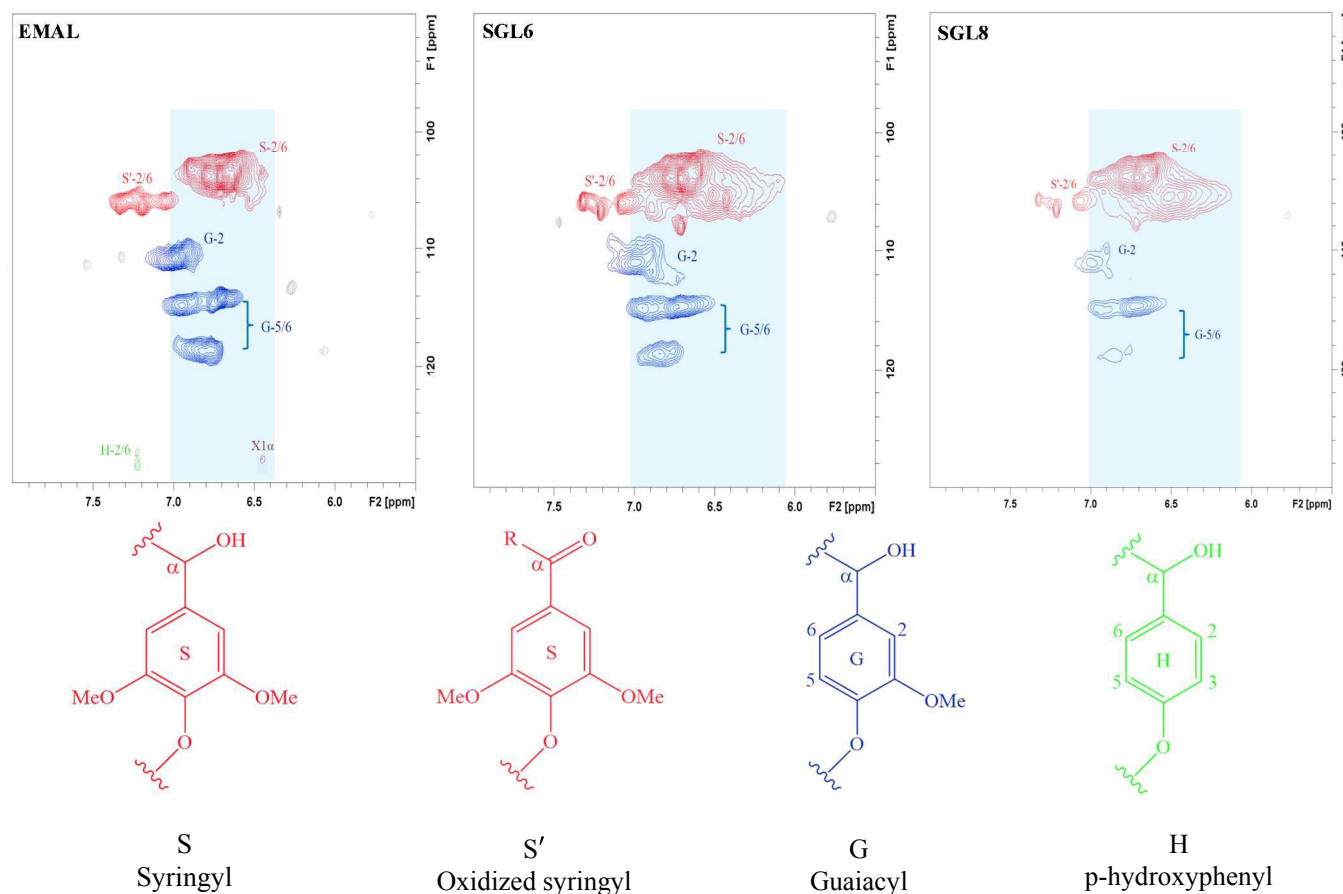




**Fig. 4** HSQC of EMAL and isolated GTP lignin – aromatic region (SGL6: recovered sweet gum lignin at GTP severity  $\log(R_0)=4.61$ ; SGL8: recovered sweet gum lignin at GTP severity  $\log(R_0)=5.03$ ).

**Table 4** S/G ratio calculated from HSQC aromatic region for EMAL and GTP lignin.

Sample ID	$\log(R_0)$	S/G ratio
EMAL	/	3.2
SGL 6	4.61	4.1
SGL 8	5.03	7.6

SGL6: recovered sweet gum lignin at GTP severity  $\log(R_0)=4.61$ ; SGL8: recovered sweet gum lignin at GTP severity  $\log(R_0)=5.03$ .

**Aliphatic side chain region ( $\delta_C/\delta_H$  50-90/2.5-5.7 ppm)**

Fig. 5 displays the aliphatic region of EMAL and GTP lignin. From these spectra, the common linkages in the lignin structure exhibited well-resolved correlations. It is widely accepted that  $\beta$ -O-4 linkages (substructure A) are the most abundant in lignin coupled with small amounts of phenylcoumaran  $\beta$ -5 (substructure B), resinol  $\beta$ - $\beta$  (substructure C), and spirodienone  $\beta$ -1 (substructure D), with the cinnamyl alcohol end groups (substructure X1) as revealed through HSQC.<sup>52</sup> Semi-quantitative characterization of the different lignin linkages and cinnamyl alcohol end groups indicated the changes in bonds and end-groups after GTP processing (Table 5).

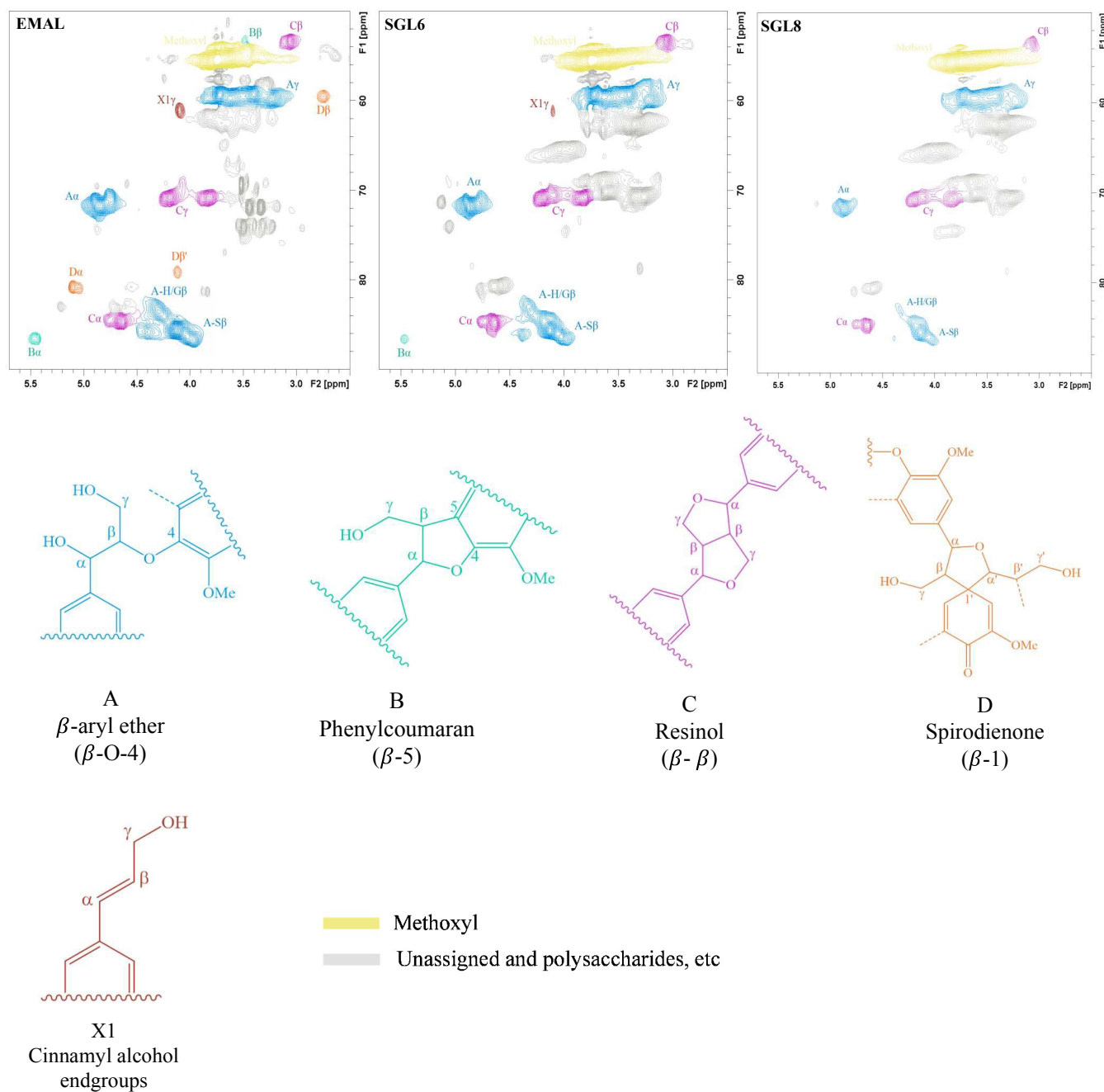


**Fig. 5** HSQC of EMAL and isolated GTP lignin – aliphatic region (SGL6: recovered sweet gum lignin at GTP severity  $\log(R_0)=4.61$ ; SGL8: recovered sweet gum lignin at GTP severity  $\log(R_0)=5.03$ ).

**Table 5** Molar abundance (per 100C9) of side chain linkages and end-groups in lignin.

Sample ID	log (R <sub>0</sub> )	β-O-4	β-5	β-β	Cinnamyl alcohol
EMAL	-	58.6	2.4	17.6	3.4
SGL 6	4.61	28.8	0.9	13.2	0.7
SGL 8	5.03	15.5	0.0	10.1	0.0

SGL6: recovered sweet gum lignin at GTP severity log(R<sub>0</sub>)=4.61; SGL8: recovered sweet gum lignin at GTP severity log(R<sub>0</sub>)=5.03; semi-quantitative analysis of β-O-4, β-5 and β-β was based on the integration of C<sub>α</sub>-H correlation; semi-quantitative analysis of cinnamyl alcohol was based on the integration of C<sub>γ</sub>-H correlation.

Consistent with a reduction in the number of β-O-4 bonded S- and G- units observed in the thioacidolysis data, the number of β-O-4 linkages decreased with increasing GTP severity. Compared to the abundance of β-O-4 linkages in EMAL, only 26% of these bonds remained after high severity GTP processing, similar to the dramatic reduction seen in the thioacidolysis data. Such a large decrease in β-O-4 linkages was also reported for lignin isolated from steam-exploded aspen.<sup>13</sup>

In addition to the extensive cleavage of β-O-4 linkages, the abundance of β-β and β-5 interunit bonds also decreased in the GTP lignin with increasing pretreatment severity. The spirodienone β-1 structure was observed in sweet gum EMAL, similarly to that observed in other hardwood native lignins.<sup>53</sup> However, its correlation disappeared in the recovered GTP lignin indicating the unlikely formation of β-1 branched structure during processing. In Fig. 5 a conspicuous cross peak was found for the GTP lignins (both SGL6 and SGL8) at ~66ppm/4.1ppm. Integrating this area accounted for 19.9/100C9 for SGL6 and 37.6/100C9 for SGL8. Based on simple peak fitting with ChemBioDraw Ultra the carbon signal arises from a primary or secondary carbons closely associated with an electronegative hydroxyl group next to another carbon attached with

an electronegative group such as a hydroxyl or carbonyl. Hence, there is a new signal arising from carbons associated primarily with rearrangements of the propyl side chain and the magnitude of the signal is related to the loss of the  $\beta$ -O-4 linkages.

### Molecular weight of GTP lignin

Based on the destruction of native interunit linkages during GTP processing, lignin was expected to decrease in molecular weight significantly compared to EMAL. The relative molecular weight of isolated GTP lignin was determined by size exclusion chromatography (SEC) using a universal calibration method. Lignin relative molecular weight was plotted as a function of GTP severity for both the number average ( $M_n$ ) and weight average ( $M_w$ ) molecular weights to elucidate relative changes arising from the GTP processing (Fig. 6).

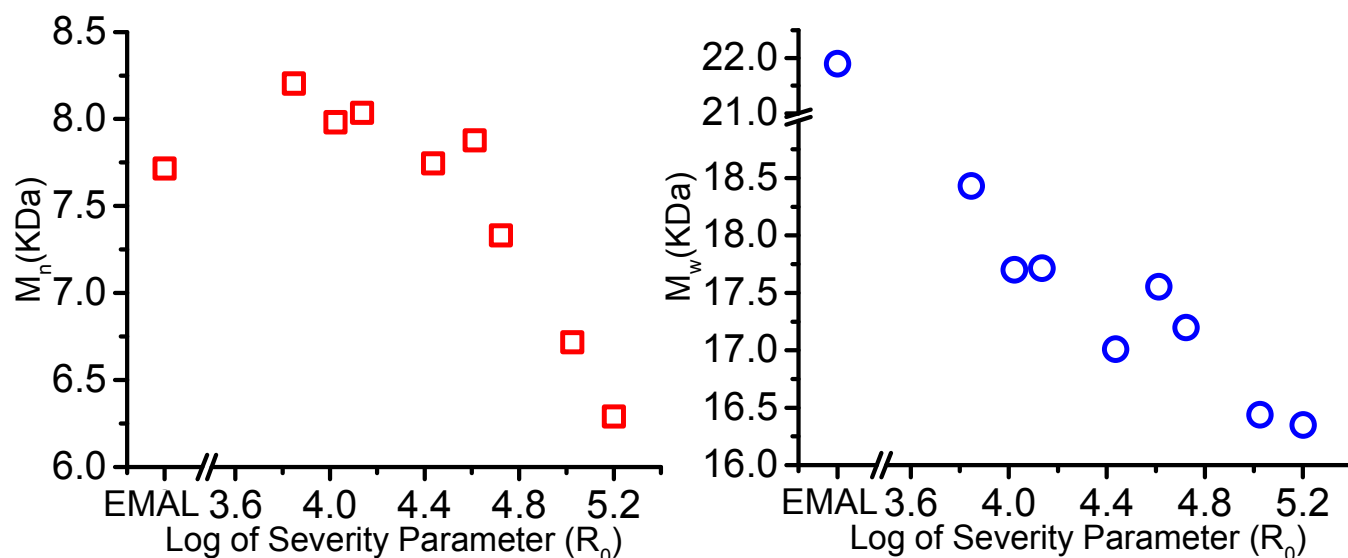


**Fig. 6** Relative molecular weight of EMAL and isolated GTP lignin as a function of the severity parameter,  $\log(R_0)$ .

For  $M_n$ , there was an initial increase relative to the EMAL control followed by a linear decrease for all remaining GTP lignin severity levels. At the highest pretreatment severity, a small decrease of 1500 Da in  $M_n$  was observed for GTP lignin compared to EMAL. This result

was surprising relative to the extensive decomposition of native lignin linkages as revealed in the thioacidolysis and 2-D NMR results. Thus, thermally induced coupling occurred in the GTP lignin that compensated the extensive scission of bonds. Direct evidence for this was found with an increase in C<sub>5</sub> condensed units as indicated by the <sup>31</sup>P-NMR data, however this only corresponded to approximately 4 to 8 new linkages per 100 C<sub>9</sub>. The resulting GTP lignin still showed relatively high M<sub>n</sub> after extensive alkyl aryl ether bond breakage. However, unlike the increase in M<sub>n</sub> after steam explosion due to the extensive C-C condensation when GTP severities were above log(R<sub>0</sub>)=3.2, there was no M<sub>n</sub> increase as GTP processing severity increased. Although GTP processing occurred at relatively high temperatures, lignin depolymerization was still predominant. Additionally, the M<sub>w</sub> decreased at higher severity factors, even relative to EMAL. Interestingly, the data revealed a small polydispersity index for GTP lignin in the range of 2.2 to 2.6, with even a smaller variance than that of EMAL (PDI = 2.8 for EMAL). This smaller PDI was unusual for processes involving both lignin depolymerization and repolymerization processes. These results are noteworthy and in contrast to relative changes reported in the literature for lignin isolated from steam-explosion or other steam treatments at comparable severities. Upon inspection of the correlations between molecular weight characteristics and free syringyl hydroxyl groups (Supporting information Fig. S4) there seems to be a controlled depolymerization process, which suggests a pathway that leads to specific coupling reactions during the depolymerization of β-O-4 and repolymerization process for this system.

### Thermal analysis of GTP lignin

The thermal stability and the glass transition temperature of the recovered GTP lignin was determined by TGA and DSC (example curves shown in Supporting Information). As shown in

Table 6, the lignin degradation temperature ( $T_d$ ) at 5% weight loss increased as a function of GTP processing severity. GTP processing of wood introduced an initial heat treatment on lignin. Cui et al. revealed that  $T_d$  increased for isolated lignin when heated above its glass transition temperature.<sup>7</sup> GTP lignin displayed significantly greater thermal stability compared to other previously reported lignins,<sup>54-56</sup> even greater than fully derivatized kraft lignins.<sup>7</sup> This property would limit off-gassing during processing, but in light of the structural changes induced through heating revealed above, caution should be noted arising from structural rearrangement.

A consistent glass transition temperature for the isolated GTP lignin (Table 6) was observed, which was not significantly impacted by GTP pretreatment. These values were the same for either the initial heating ramp or the second heating ramp, suggesting some stability of structure. Prior reports indicated  $T_g$  values for several commercial lignins:<sup>57-59</sup> organosolv lignin had a  $T_g$  of 106 °C, lignosulfonates had a  $T_g$  of 105 °C and  $T_g$  for kraft and steam-exploded lignin was around 175 and 93 °C, respectively. Compared to these values, lignin isolated from GTP pretreated sweet gum had a relatively higher glass transition temperature (162-170 °C). Polymer mobility is impacted by the structure and functionality of the molecule. For lignin, functionality such as hydroxyl groups significantly impact the  $T_g$ .<sup>59</sup> Based on the invariance of the  $T_g$  data for the 6 severities tested, it appears that the lowest severity level provides a critical modification level. The higher thermal stability of lignin isolated from GTP pretreated biomass, with a high glass transition temperature, suggests potential application of this material in engineering thermoplastics.<sup>1, 58</sup> Additional studies are required to investigate the stability of its melt rheology, however the data suggests the pretreatment modifies lignin in a manner useful for polymer applications that can either benefit from the large amounts of free phenolic groups and/or can be blended at higher temperatures. It is unknown how GTP processing impacts the mechanical

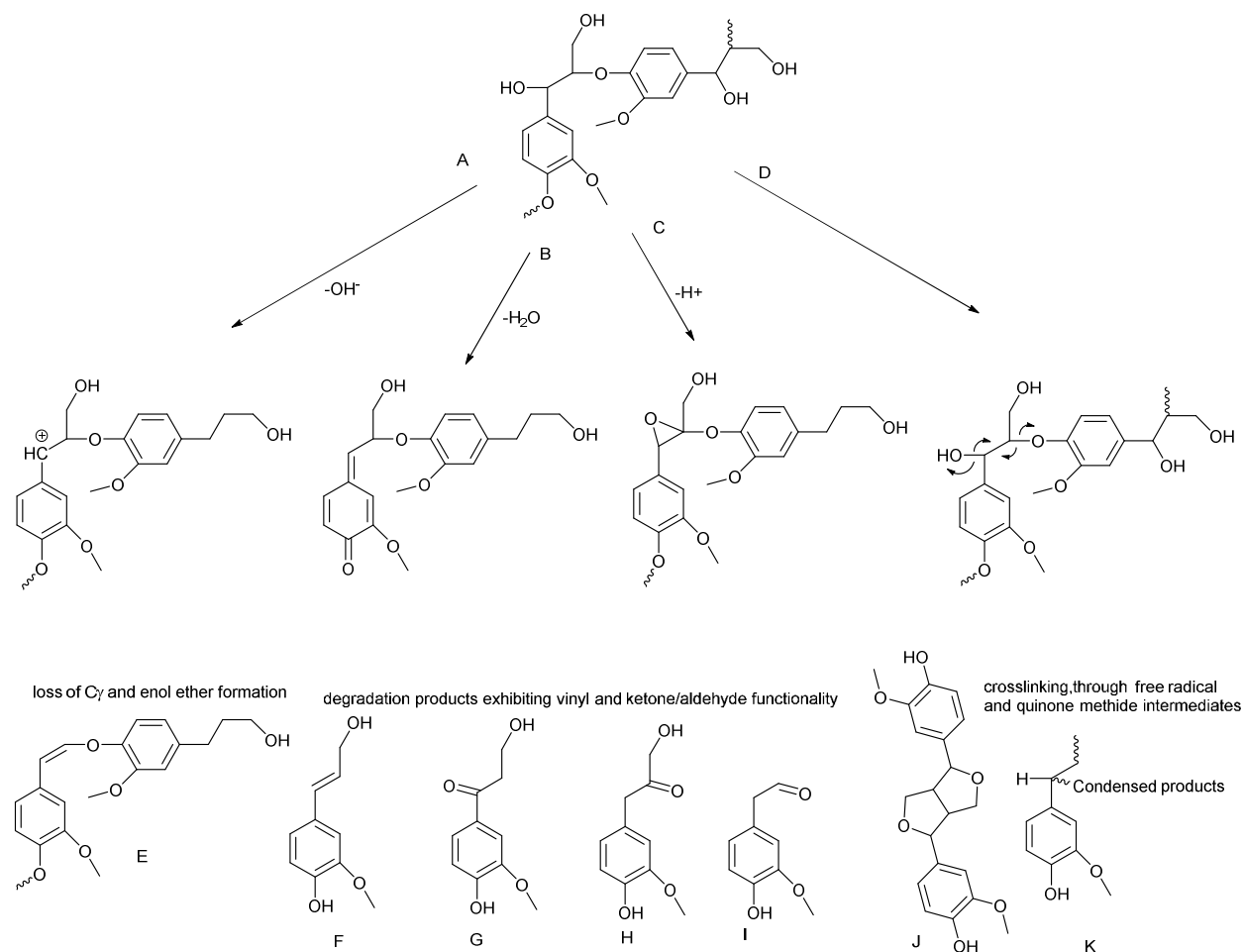
properties of lignin, however, dynamic mechanical analysis of fractionated lignin has shown that the glassy shear modulus of lignin is not impacted by the various lignin structures and the differences in structure mainly influence the rubbery plateau.<sup>60</sup> Because of the minimum impact of structure on the glassy region, it is expected that the GTP lignin would have similar behavior.

**Table 6** Degradation temperature and glass transition temperature of GTP lignin.

log(R <sub>0</sub> )	T <sub>g</sub> (°C)	T <sub>d</sub> (°C)
EMAL	ND	201.6
4.14	162.8 (0.2)	248.1(2.1)
4.44	166.4 (0.2)	276.6 (2.8)
4.61	165.9 (0.3)	282.1 (2.1)
4.72	164.5 (1.2)	288.2 (2.7)
5.03	166.2 (0.1)	292.9 (5.8)
5.20	169.5 (0.5)	296.8 (9.5)

T<sub>d</sub> was analyzed at 5% weight loss; ND: not determined; parentheses indicate standard deviation from duplicates.

## Discussion

**Scheme 1** Lignin degradation pathway and produced structures.

Extensive scission, up to three quarters of  $\beta$ -O-4 linkages, occurred in the lignin recovered from GTP pretreatment. As a result, phenolic hydroxyl content increased correspondingly to linkage breakage of these labile ethers. Yet there was minimal depolymerization of the lignin as revealed by GPC. The question arises of the exact mechanism of breakdown and repolymerization of the lignin. While other pretreatments such as steam-explosion occur in the presence of acids such as acetic acid typically formed from hemicellulose during steam-explosion,<sup>61</sup> glycerol thermal processing provided a water extract that was only slightly acidic (pH 5).<sup>23</sup> Typically, any residual



acids present may give rise to a traditional thermo-solvolysis route where, there is loss of the alpha hydroxyl forming a benzylic carbocation (Scheme 1A) that can be a) etherified with glycerol leading to cleavage of the  $\beta$ -O-4 linkages and a variety of degradation products or b) forms an enol ether structure (1E) with release of C $\gamma$ . However, the solvolysis pathway results in significant formation of conjugated carbonyl groups at the C $\alpha$  (1G), and the recovered lignin revealed minimal oxidation at C $\alpha$  in the 2D-NMR compared to the EMAL lignin. Additionally, FTIR analysis showed a dramatic decrease in the absorbance of the conjugated ketone (Supporting information Fig. S5), as well as a significant signal from the benzylic hydrogen in the  $^1\text{H}$  NMR data (supporting information Fig. S1). Additionally, elimination of C- $\gamma$  OH during enol ether formation would result in formaldehyde release. The enol ether structures may not be stable in the GTP processing environment or in the recovery during lignin acid precipitation, which further results in the production of free phenolics<sup>36</sup> and aldehyde end groups (1I) along with the possibility of unconjugated ketones at the C $\beta$  (1H). Hence, solvolysis can only be a limited part of the mechanism as there are not conjugated carbonyl products and limited acid present to catalyze the reaction.

We hypothesize that thermal induced decomposition of  $\beta$ -O-4 is a key mechanism occurring during GTP processing of biomass and this can occur via quinone methide intermediates<sup>62</sup> (loss of H/OH, Scheme 1B), oxirane intermediates<sup>49</sup> (loss of H $^+$ , Scheme 1C), and/or free radical cleavage<sup>63</sup> (Scheme 1D). Cleavage of  $\beta$ -O-4 through the various pathways, results in the formation of lignin molecules with free vinylic units such as cinnamyl alcohol (1F).<sup>37</sup> However, in the present study, the number of cinnamyl alcohol end-groups also decreased after GTP processing and even disappeared after high severity GTP processing (2D-NMR data). Thus, if homolytic cleavage is the primary mechanism associated with the extensive  $\beta$ -O-4 cleavage

observed, the products produced are transient at high temperatures. In support of this case, it has been reported that homolytic cleavage products can form  $\beta$ - $\beta$  pinosresinol and syringaresinol structures (1J) which would occur from repolymerization of the vinyl groups.<sup>64, 65</sup> Other repolymerization routes involve the benzylic carbons, from quinone methide intermediates leading to condensed structures (1K).

Furthermore, for thermal decomposition mechanisms, lignin interunit structure greatly impacts the reactions when comparing etherified lignin units vs. free phenolic units. The latter has a lower thermal decomposition temperature, possibly directing decomposition to certain lignin units. Specifically, Brežný et al.<sup>66</sup> reported low temperature thermolysis for  $\beta$ -O-4 phenolic model compounds in 190-200 °C and etherified analogs at 250-260 °C, demonstrating the difference in sensitivity between these compounds. With a difference in decomposition temperatures, the processing should result from an end-wise depolymerization of the lignin from free phenolic ends. Additionally, the different hydrogen bonds formed by C- $\gamma$  hydroxyl groups are critical in impacting the  $\beta$ -O-4 thermal cleavage mechanism.<sup>36</sup> According to Kawamoto et al.,<sup>67</sup> the side-chain hydroxyl groups, especially on the C- $\gamma$  position, play a key role in the pyrolytic cleavage mechanism of the  $\beta$ -O-4 linkage. For the C- $\gamma$  deoxyl types, the  $\beta$ -O-4 linkages are cleaved through a radical chain mechanism, but high temperatures in the range of 400 °C are necessary for thermolysis.<sup>62</sup> However, the C- $\gamma$  hydroxyl type possesses a higher reactivity, which requires a lower thermal energy for  $\beta$ -O-4 breakage. Haw and Schultz<sup>68</sup> reported that thermal decomposition of  $\beta$ -O-4 linkages initiated at 220 °C for the C- $\gamma$  hydroxyl type. Hence, while glycerol (and other high molecular weight or multifunctional alcohols) is often used as a plasticizer in compounding to protect from dehydration reactions in biopolymers, for lignin, the addition of glycerol may serve to catalyze the homolytic cleavage of lignin.

## Conclusions

Non-catalytic glycerol thermal pretreatment (GTP) was studied as a means for isolation and recovery of lignin and to examine the sensitivity of native lignin to heat. Processing biomass at moderately severe temperatures of 200 to 240 °C in an anhydrous environment for short times with a hydrogen bonding solvent gave rise to significant changes in lignin structure. After GTP pretreatment, 41% of the initial Klason lignin in the biomass input was recovered in a powdered form without any catalyst using aqueous dioxane extraction at room temperature. Further structural investigation of the isolated lignin indicated that glycerol thermal processing facilitated aliphatic hydroxyl reduction and extensive  $\beta$ -O-4 bond decomposition resulting in phenolic hydroxyl liberation. The syringyl phenolic functionality of the GTP lignin increased linearly with the log of the severity parameter due to alkyl aryl ether bond cleavage. The amount of phenolic hydroxyl content was considerably higher than other lignins at similar levels of delignification. Condensation of the lignin also occurred causing the GTP lignin to have a relatively high molecular weight, near to that of enzymatic mild acidolysis lignins. The resulting GTP lignin was significantly more thermally stable, with a glass transition temperature that was invariant to GTP processing severity. As these temperatures and processing times border on the thermal processing of many thermoplastic polymers, the study provided extensive evidence for the structural changes that can occur in lignin at high temperatures in so called benign environments.

## Experimental

### General

Chemicals and reagents used in this research were purchased from Sigma-Aldrich, Alfa Aesar and MP Biomedicals and used as received. A mature hardwood sweet gum (*Liquidambar*

*styraciflua*) was adopted as the biomass resource in this research. Preparation of biomass samples was performed as reported previously.<sup>23</sup>

### **Glycerol thermal processing (GTP)**

The biomass was pretreated at nine severities ( $R_0$ ), ranging from 200 to 240 °C and from 4 to 12 min according to a previous report.<sup>23</sup> The severity parameter combines both time and temperature into an empirical reaction model, represented as a logarithmic scale, describing the thermo-mechanical hydrolysis of biomass.<sup>69, 70</sup> The GTP pretreated biomass was collected and stored at 4 °C for further analysis.

### **Lignin isolation from pretreated biomass**

GTP pretreated sweet gum (GTPSG) was first water extracted to remove the additional glycerol residue and degraded components before lignin isolation.<sup>23</sup> Solvent extraction of thoroughly dried water-extracted GTPSG was performed using 96% (v/v) 1,4-dioxane<sup>71</sup> (azeotrope) at a solid to liquid ratio of 1/25 with continuous stirring at ambient temperature without catalysts. After a 24 hour extraction, the residual biomass was collected through filtration and the filtrate was further passed through a 10  $\mu$ m glassy-fiber filter to remove any biomass solids before concentrating to <100 ml under reduced pressure. The concentrated solvent extract was added dropwise into 1 L 0.01 M hydrochloride acid<sup>72</sup> (pH=2) for lignin precipitation. After settling overnight at 4 °C, the precipitated lignin was collected through centrifugation and further rinsed 3 times with deionized water before freeze-drying. The recovered lignin, labeled as GTP lignin, was freeze-dried for mass balance calculations. Compositional analysis of GTP biomass before and after solvent extraction was performed according to the NREL standard.<sup>73</sup>

The GTP lignin recovery yield relative to the total initial lignin in the original biomass was calculated through Eq 1.

$$\text{recovered lignin yield}\% = \frac{m_{\text{rec lignin}}}{m_0 \times \text{Klignin}_0} \times 100\% \quad (\text{Eq1})$$

$m_{\text{rec lignin}}$  : dry mass of recovered GTP lignin for specific biomass input to pretreatment;

$m_0$  : total dry mass of biomass input to GTP pretreatment;

$\text{Klignin}_0$  : Klason lignin content in biomass input.

Enzymatic mild acidolysis lignin (EMAL) from extractive free sweet gum was used as a reference for the GTP process because no lignin could be extracted from untreated biomass with DMF.<sup>72</sup>

### GTP lignin elemental analysis

Elemental analysis (carbon, hydrogen and nitrogen) of isolated GTP lignin was determined on automatic analyzers comprised of Perkin-Elmer Model 2400 Series II autoanalyzers, LECO CHNS-932 Analyzers, Carlo Erba Model 1108 Analyzers and Costech ECS. Results were reported as weight percentage of biomass dry weight (C%, H% and N%). Oxygen content (O%) was calculated by subtracting the composition fraction of the carbon, hydrogen, and nitrogen from unity.

### GTP lignin acetylation and quantitative $^1\text{H}$ -NMR

Lignin acetylation was conducted according to the procedure of Glasser et al.<sup>74</sup> with slight modification. 100 mg dried lignin (GTP lignin or EMAL) was dissolved in 3 ml anhydrous pyridine followed by the addition of an equal volume of anhydrous acetic anhydride. The reaction was performed at room temperature for 24 hours in a nitrogen atmosphere with continuous stirring. Then, the reaction mixture was added dropwise into 200 ml 0.01 N hydrochloric acid. The acetylated lignin was collected through filtration using a 10  $\mu\text{m}$  nylon filter and then rinsed using 0.01 N hydrochloric acid 3 times to remove any solvent residue,

followed by a 3x deionized water wash. The resulting lignin was freeze-dried followed by vacuum drying.

20 mg of acetylated lignin was fully dissolved in 500  $\mu$ l chloroform- $d_6$ . An internal standard for NMR quantification was prepared by dissolving 20 mg 2,3,4,5,6-pentafluorobenzaldehyde (PFB) in 1.5 ml chloroform- $d_6$ . Then, 200  $\mu$ l PFB solution was added into the lignin solution before transferring to a 5 mm NMR tube. The  $^1\text{H}$ -NMR was collected on a Bruker Avance II 500 MHz multinuclear spectrometer with a pulse angle of  $30^\circ$  and pulse delay time of 7 s. 32 scans were acquired and the spectra were processed using MestReNova software. All chemical shifts were reported according to TMS internal reference at 0 ppm. Peak assignments of quantitative  $^1\text{H}$ -NMR are shown in supporting information Fig. S1 according to previous reports.<sup>75-78</sup>

#### **Quantitative $^{31}\text{P}$ -NMR analysis of recovered GTP lignin**

Quantitative phosphorous-31 nuclear magnetic resonance spectroscopy ( $^{31}\text{P}$ -NMR) analysis was performed on a Varian INOVA 400 MHz multinuclear spectrometer at a frequency of 162.07 MHz for  $^{31}\text{P}$  spins. This method was adapted from reports by Argyropoulos and co-workers.<sup>29, 39, 79-82</sup> Prior to analysis, all lignin samples were stored in a vacuum oven for 48 hours.

A solvent mixture composed of pyridine/chloroform- $d_6$  ( $\text{CDCl}_3$ ) with a ratio of 1.6/1 (v/v) was freshly prepared for  $^{31}\text{P}$ -NMR. Endo-N-hydroxy-5-norbornene-2,3-dicarboximide (e-HNDI) was chosen as an internal standard,<sup>83</sup> which was prepared at a concentration of 11.32 mg/ml from the above solvent mixture, pyridine/ $\text{CDCl}_3$  (1.6/1). Chromium (III) acetylacetonate ( $\text{Cr}(\text{acac})_3$ ) as the spin relaxation reagent<sup>84</sup> was prepared in  $\text{CDCl}_3$  at a concentration of 10 mg/ml. 30 mg of GTP lignin or EMAL was dissolved in 500  $\mu$ l of the above solvent mixture followed by adding 200  $\mu$ l e-HNDI solution and 50  $\mu$ l  $\text{Cr}(\text{acac})_3$  solution. The solution was thoroughly mixed using a vortex mixer. Then, 100  $\mu$ l 2-chloro-4,4,5,5-tetramethyl-1,3,2-dioxaphospholane (PR(II)) was added as

the phosphitylation reagent followed by extensive vortex mixing. The final solution was immediately transferred to a 5 mm NMR tube and quantitative  $^{31}\text{P}$ -NMR spectra were acquired immediately. Specific spectra acquisition parameters were as follows: a pulse angle of  $90^\circ$  and pulse delay time of 5 seconds was chosen to improve signal to noise ratio as well as full relaxation; spectra width was 33999.2 Hz; to avoid peak splitting effects, an inverse-gated decoupling on proton spins was applied. Quantitative spectra were collected without Nuclear Overhauser Effect. 256 scans were collected for each sample and subsequently the spectra were processed using MestReNova software. Signal to noise ratio was improved using signal apodization: exponential 3.0 Hz with additional Gaussian 1.0 GB. Zero filling was 256 K. All chemical shifts were reported relative to the sharp peak of the phosphitylated water (residual moisture) at 132.2 ppm.

Peak assignments of quantitative  $^{31}\text{P}$ -NMR are shown in supporting information Fig. S2, based on previous reports.<sup>39, 83</sup> It should be noted that syringyl phenolic groups were integrated separately from the  $\text{C}_5$  condensed units based on literature.<sup>39</sup>

### **Lignin thioacidolysis-gas chromatography (GC)**

Thioacidolysis of completely dried GTP lignin was performed according to the report by Rolando et al.<sup>85</sup>

GC analysis of trimethylsilylated thioacidolysis products was performed on an Agilent gas chromatograph (GC) equipped with a polydimethylsiloxane fused silica capillary column (30 m x 320  $\mu\text{m}$ , length x I.D., with 0.25  $\mu\text{m}$  film thickness). GC conditions were: Injector port  $280^\circ\text{C}$  with a sample flow rate of 1 ml/min. The oven temp was ramped from  $200^\circ\text{C}$  to  $260^\circ\text{C}$  at  $4^\circ\text{C}/\text{min}$  and then increased to  $300^\circ\text{C}$  at  $30^\circ\text{C}/\text{min}$ . Detection was performed with a flame ionization detector (FID) at  $300^\circ\text{C}$ . Hydrogen was used as the carrier gas with a flow rate of 30

ml/min. 1  $\mu$ l of silylated sample was manually injected and the resulting chromatograms were analyzed using OpenLAB CDS ChemStation software.

### **Two-dimensional $^{13}\text{C}$ - $^1\text{H}$ heteronuclear single quantum coherence (HSQC) NMR spectroscopy of GTP lignin**

All lignin samples were prepared using DMSO- $\text{d}_6$  and sonicated until homogenous in a Branson 2510 table-top cleaner (Branson Ultrasonic Corporation, Danbury, CT). The temperature of the bath was closely monitored and maintained below 55  $^\circ\text{C}$ . The homogeneous solutions were transferred to NMR tubes. HSQC spectra were acquired at 25  $^\circ\text{C}$  using a Bruker Avance-600 MHz instrument equipped with a 5 mm inverse-gradient  $^1\text{H}/^{13}\text{C}$  cryoprobe using a Q-HSQC ETGP pulse program (ns = 200, ds = 16, number of increments = 256, d1 = 1.0 s).<sup>86, 87</sup> Gaussian apodization in F2 (LB = -0.18, GB = 0.005) and squared cosine-bell in F1 (LB = -0.10, GB = 0.001) was applied prior to 2D Fourier Transformation. Chemical shifts were referenced to the central DMSO peak at 39.5/2.5 ppm ( $\delta_{\text{C}}/\delta_{\text{H}}$ ). Assignments of the HSQC spectra were described elsewhere.<sup>43, 44</sup> A semi-quantitative analysis of the volume integrals of the HSQC correlation peaks was performed using Bruker's Topspin 2.0 processing software. Changes in lignin structure were determined based on volume integration of HSQC spectral contour correlations. The  $\text{C}_2\text{-H}_2$  position of the guaiacyl unit and the  $\text{C}_{2,6}\text{-H}_{2,6}$  positions in the syringyl unit were considered to be stable<sup>50</sup> and used as the internal standard that represents aromatic  $\text{C}_9$  units in the lignin. Spectra integration was performed on the same contour level. All integrals displayed less than 10% error (based on the use of organosolv lignin in triplicate – data not shown), confirming the precision of the quantification from 2D HSQC spectra.

### **Gel permeation chromatography of recovered lignin**



Lignin solutions, 1% (w/v), were prepared in analytical-grade 1-methyl-2-pyrrolidinone (NMP). The polydispersity of dissolved lignin was determined using analytical techniques involving SEC UV-A290 as previously described.<sup>88</sup> An Agilent 1200 series binary LC system (G1312B) equipped with diode-array (G1315D) detector was used. Separation was achieved with a Mixed-D column (5  $\mu$ m particle size, 300 mm x 7.5 mm i.d., linear molecular mass range of 200 to 400,000 u, Agilent Technologies Inc.) at 80 °C using a mobile phase of NMP at a flow rate of 0.5 ml/min. Absorbance of materials eluting from the column was detected using UV-A absorbance ( $\lambda$ =290 nm). The GPC chromatograms are shown in the supporting information Fig. S3. Spectral intensities were area-normalized and relative molecular mass was determined after calibration of the system with polystyrene standards.

### **Thermal analysis of GTP lignin**

The thermal degradation temperature of dried isolated lignin was studied by thermogravimetric analysis (TGA) on a TA instruments Q100 with a heating rate of 10 °C/min from ambient temperature to 900 °C for complete degradation in air. Initial degradation temperatures were determined at 5% weight loss.

The glass transition temperature ( $T_g$ ) of lignin was determined on a TA Instruments Q100 differential scanning calorimeter (DSC). The heating rate was 5 °C/min over a temperature range of 25 to 200 °C in a nitrogen atmosphere. Cycles of heat/cool/heat were performed and  $T_g$  was analyzed as the midpoint of the heat capacity transition on the first heating.

### **Acknowledgments**

The authors greatly acknowledge financial support from USDA NIFA 2010-65504-20429 for the work along with support from the Institute for Critical Technology and Science at Virginia Tech and the Virginia Tech Graduate School. Additionally, a portion of the work conducted by the Joint BioEnergy Institute was supported by the Office of Science, Office of Biological and Environmental Research, of the U.S. DOE under contract no. DE-AC02-05CH11231. NS was supported by the National Science Foundation under Cooperative Agreement No. 1355438

## Abbreviations

GTP, glycerol thermal processing; SG, extractive-free sweet gum; EMAL, enzymatic mild acidolysis lignin; SGL, sweet gum lignin isolated from glycerol thermal pretreated biomass; PDI, polydispersity index.

## References

1. J. H. Lora and W. G. Glasser, *J Polym Environ*, 2002, **10**, 39-48.
2. F. S. Chakar and A. J. Ragauskas, *Industrial Crops and Products*, 2004, **20**, 131-141.
3. T. Q. Hu and B. R. James, in *Chemical Modification, Properties, and Usage of Lignin*, ed. T. Q. Hu, Springer US, New York, 2002, pp. 247-265.
4. W. O. Doherty, P. Mousavioun and C. M. Fellows, *Industrial Crops and Products*, 2011, **33**, 259-276.
5. K. V. Pillai and S. Rennecker, *Biomacromolecules*, 2009, **10**, 798-804.
6. W. Thielemans and R. P. Wool, *Biomacromolecules*, 2005, **6**, 1895-1905.
7. C. Cui, H. Sadeghifar, S. Sen and D. S. Argyropoulos, *BioResources*, 2013, **8**, 864-886.
8. N. S. Cetin and N. Özmen, *International Journal of Adhesion and Adhesives*, 2002, **22**, 477-480.
9. S. S. Kelley, W. G. Glasser and T. C. Ward, *Polymer*, 1989, **30**, 2265-2268.

10. T. G. Rials and W. G. Glasser, *J Appl Polym Sci*, 1989, **37**, 2399-2415.
11. V. B. Agbor, N. Cicek, R. Sparling, A. Berlin and D. B. Levin, *Biotechnol Adv*, 2011, **29**, 675-685.
12. H.-J. Huang, S. Ramaswamy, U. W. Tschirner and B. V. Ramarao, *Separation and Purification Technology*, 2008, **62**, 1-21.
13. J. Li, G. Henriksson and G. Gellerstedt, *Bioresource technology*, 2007, **98**, 3061-3068.
14. M. M. Ibrahim, F. A. Agblevor and W. K. El-Zawawy, *Bioresources*, 2010, **5**, 397-418.
15. H. Janshekar and A. Fiechter, in *Pentoses and Lignin*, eds. H. Janshekar and A. Fiechter, Springer Berlin Heidelberg, New York, 1983, pp. 119-178.
16. P. Sannigrahi, A. J. Ragauskas and S. J. Miller, *Energy Fuel*, 2010, **24**, 683-689.
17. J. L. McCarthy and A. Islam, in *Lignin : Historical, Biological, and Materials Perspectives*, eds. W. G. Glasser, R. A. Northey and T. P. Schultz, ACS Symposium Series, Washington, DC, 2000, vol. 742, pp. 2-99.
18. Demirbas, *Bioresource technology*, 1998, **63**, 179-185.
19. A. Demirbas, *Energy Sources, Part A: Recovery, Utilization, and Environmental Effects*, 2008, **30**, 1120-1126.
20. M. M. Küçük, *Energy Source*, 2005, **27**, 1245-1255.
21. C. Vanasse, E. Chornet and R. Overend, *The Canadian Journal of Chemical Engineering*, 1988, **66**, 112-120.
22. J. R. Barone, W. F. Schmidt and C. F. Liebner, *Journal of applied polymer science*, 2005, **97**, 1644-1651.
23. W. Zhang, J. R. Barone and S. Renneckar, *ACS Sustainable Chemistry & Engineering*, 2015, **3**, 413-420.
24. W. Zhang, N. Sathitsuksanoh, J. R. Barone and S. Renneckar, *Bioresource technology*, 2016, **199**, 148-154.
25. L. P. Novo, L. V. A. Gurgel, K. Marabezi and A. A. D. Curvelo, *Bioresource technology*, 2011, **102**, 10040-10046.
26. S. Chowdhury and C. E. Frazier, *Biomacromolecules*, 2013, **14**, 1166-1173.
27. R. W. Thring, E. Chornet and R. P. Overend, *Biomass*, 1990, **23**, 289-305.

28. Y. Archipov, D. S. Argyropoulos, H. I. Bolker and C. Heitner, *Journal of Wood Chemistry and Technology*, 1991, **11**, 137-157.
29. D. S. Argyropoulos, *Journal of Wood Chemistry and Technology*, 1994, **14**, 45-63.
30. R. Brezny, V. Mihalov and V. Kovacik, *Holzforschung*, 1983, **37**, 199-204.
31. T. J. McDonough, *IPST technical paper series*, 1992, 1-17.
32. Y. Liu, S. Carriero, K. Pye and D. S. Argyropoulos, in *Lignin: Historical, Biological, and Materials Perspectives*, eds. W. G. Glasser, R. A. Northey and T. P. Schultz, ACS Symposium Series, Washington, DC, 1999, pp. 447–464.
33. E. Jakab, O. Faix and F. Till, *J Anal Appl Pyrol*, 1997, **40**, 171-186.
34. M. R. Sturgeon, S. Kim, K. Lawrence, R. S. Paton, S. C. Chmely, M. Nimlos, T. D. Foust and G. T. Beckham, *ACS Sustainable Chemistry & Engineering*, 2013, **2**, 472-485.
35. E. Jakab, O. Faix, F. Till and T. Székely, *J Anal Appl Pyrol*, 1995, **35**, 167-179.
36. H. Kawamoto and S. Saka, *Journal of Wood Chemistry and Technology*, 2007, **27**, 113-120.
37. H. Kawamoto, S. Horigoshi and S. Saka, *J Wood Sci*, 2007, **53**, 168-174.
38. A. Guerra, I. Filpponen, L. A. Lucia, C. Saquing, S. Baumberger and D. S. Argyropoulos, *Journal of agricultural and food chemistry*, 2006, **54**, 5939-5947.
39. A. Granata and D. S. Argyropoulos, *Journal of agricultural and food chemistry*, 1995, **43**, 1538-1544.
40. D. Robert, M. Bardet, C. Lapierre and G. Gellerstedt, *Cell Chem Technol*, 1988, **22**, 221-230.
41. M. Funaoka, T. Kako and I. Abe, *Wood Science and Technology*, 1990, **24**, 277-288.
42. L. L. Landucci, *Search for lignin condensation reactions with modern NMR techniques*, American Chemical Society, Washington, DC, 1989.
43. H. Kim and J. Ralph, *Organic & Biomolecular Chemistry*, 2010, **8**, 576-591.
44. D. J. Yelle, J. Ralph and C. R. Frihart, *Magn Reson Chem*, 2008, **46**, 508-517.
45. M. Bunzel and J. Ralph, *Journal of agricultural and food chemistry*, 2006, **54**, 8352-8361.

46. D. Ibarra, M. I. Chavez, J. Rencoret, J. C. del Río, A. Gutierrez, J. Romero, S. Camarero, M. J. Martínez, J. Jiménez-Barbero and A. T. Martinez, *Holzforschung*, 2007, **61**, 634-646.
47. D. Ibarra, M. I. Chávez, J. Rencoret, J. C. Del Río, A. Gutiérrez, J. Romero, S. Camarero, M. J. Martínez, J. Jiménez-Barbero and A. T. Martínez, *Journal of agricultural and food chemistry*, 2007, **55**, 3477-3490.
48. J. Rencoret, G. Marques, A. Gutierrez, L. Nieto, J. I. Santos, J. Jimenez-Barbero, A. T. Martinez and J. C. del Rio, *Holzforschung*, 2009, **63**, 691-698.
49. J. Rencoret, A. Gutiérrez, L. Nieto, J. Jiménez-Barbero, C. B. Faulds, H. Kim, J. Ralph, Á. T. Martínez and C. José, *Plant Physiol*, 2011, **155**, 667-682.
50. M. Sette, R. Wechselberger and C. Crestini, *Chem-Eur J*, 2011, **17**, 9529-9535.
51. C. Fernández-Costas, S. Gouveia, M. Sanromán and D. Moldes, *Biomass and Bioenergy*, 2014, **63**, 156-166.
52. J. Ralph, Marita, J. M., Ralph, S. A., Hatfield, R. D., etc. , in *Advances in Lignocellulosics Characterization*, ed. D. S. Argyropoulos, TAPPI Press, Atlanta, GA, 1999, pp. 55-108.
53. J. Rencoret, G. Marques, A. Gutiérrez, L. Nieto, J. I. Santos, J. Jiménez-Barbero, Á. T. Martínez and J. C. del Río, *Holzforschung*, 2009, **63**, 691-698.
54. A. Awal and M. Sain, *J Appl Polym Sci*, 2011, **122**, 956-963.
55. S. Kubo, Y. Uraki and Y. Sano, *Holzforschung*, 1996, **50**, 144-150.
56. P. Murugan, N. Mahinpey, K. E. Johnson and M. Wilson, *Energy Fuel*, 2008, **22**, 2720-2724.
57. D. Koullas, E. Koukios, E. Avgerinos, A. Abaecherli, R. Gosselink, C. Vasile, R. Lehnen, B. Saake and J. Suren, *Cell Chem Technol*, 2006, **40**, 719-725.
58. A. U. Buranov, K. A. Ross and G. Mazza, *Bioresource technology*, 2010, **101**, 7446-7455.
59. S. Kubo and J. F. Kadla, *Biomacromolecules*, 2005, **6**, 2815-2821.
60. O. Sevastyanova, M. Helander, S. Chowdhury, H. Lange, H. Wedin, L. Zhang, M. Ek, J. F. Kadla, C. Crestini and M. E. Lindström, *Journal of Applied Polymer Science*, 2014, **131**.

61. J. Li, G. Henriksson and G. Gellerstedt, *Applied biochemistry and biotechnology*, 2005, **125**, 175-188.
62. H. Kawamoto, M. Ryoritani and S. Saka, *J Anal Appl Pyrol*, 2008, **81**, 88-94.
63. K.-i. Kuroda, *J Anal Appl Pyrol*, 1995, **35**, 53-60.
64. S. Li, K. Lundquist and U. Westermarck, *Nord Pulp Pap Res J*, 2000.
65. M. Leschinsky, G. Zuckerstätter, H. K. Weber, R. Patt and H. Sixta, *Holzforschung*, 2008, **62**, 645-652.
66. R. Brežný, V. Mihalov and V. Kováčik, *Holzforschung-International Journal of the Biology, Chemistry, Physics and Technology of Wood*, 1983, **37**, 199-204.
67. H. Kawamoto, S. Horigoshi and S. Saka, *J Wood Sci*, 2007, **53**, 268-271.
68. J. F. Haw and T. P. Schultz, *Holzforschung-International Journal of the Biology, Chemistry, Physics and Technology of Wood*, 1985, **39**, 289-296.
69. R. P. Overend, E. Chornet and J. A. Gascoigne, *Philosophical Transactions of the Royal Society of London. Series A, Mathematical and Physical Sciences*, 1987, **321**, 523-536.
70. N. Abatzoglou, E. Chornet, K. Belkacemi and R. P. Overend, *Chemical Engineering Science*, 1992, **47**, 1109-1122.
71. T. Ikeda, K. Holtman, J. F. Kadla, H.-m. Chang and H. Jameel, *Journal of agricultural and food chemistry*, 2002, **50**, 129-135.
72. S. Wu and D. S. Argyropoulos, *J Pulp Pap Sci*, 2003, **29**, 235-240.
73. A. Sluiter, B. Hames, R. Ruiz, C. Scarlata, J. Sluiter, D. Templeton and D. Crocker, *Laboratory Analytical Procedure*, 2008, 1-15.
74. W. G. Glasser, V. Davé and C. E. Frazier, *Journal of Wood Chemistry and Technology*, 1993, **13**, 545-559.
75. C. L. Chen and D. Robert, *Method Enzymol*, 1988, **161**, 137-174.
76. K. Lundquist, in *Methods in Lignin Chemistry*, eds. S. Y. Lin and C. W. Dence, Springer, New York, 1992, pp. 242-249.
77. D. V. Evtuguin, C. P. Neto, A. M. Silva, P. M. Domingues, F. M. Amado, D. Robert and O. Faix, *Journal of agricultural and food chemistry*, 2001, **49**, 4252-4261.
78. J. Jakobsons, B. Hortling, P. Erins and J. Sundquist, *Holzforschung-International Journal of the Biology, Chemistry, Physics and Technology of Wood*, 1995, **49**, 51-59.

79. D. S. Argyropoulos, *Journal of Wood Chemistry and Technology*, 1994, **14**, 65-82.
80. D. S. Argyropoulos, *Res Chem Intermediat*, 1995, **21**, 373-395.
81. D. S. Argyropoulos, H. I. Bolker, C. Heitner and Y. Archipov, *Holzforschung*, 1993, **47**, 50-56.
82. B. Li, I. Filpponen and D. S. Argyropoulos, *Industrial & Engineering Chemistry Research*, 2010, **49**, 3126-3136.
83. M. Zawadzki and A. Ragauskas, *Holzforschung*, 2001, **55**, 283-285.
84. F. Kasler and M. Tierney, *Microchimica Acta*, 1978, **70**, 411-422.
85. C. Rolando, B. Monties and C. Lapierre, in *Methods in lignin chemistry*, eds. S. Y. Lin and C. W. Dence, Springer, New York, 1992, pp. 334-349.
86. S. Heikkinen, M. M. Toikka, P. T. Karhunen and I. A. Kilpeläinen, *J Am Chem Soc*, 2003, **125**, 4362-4367.
87. J. A. Dolan, N. Sathitsuksanoh, K. Rodriguez, B. A. Simmons, C. E. Frazier and S. Renneckar, *RSC Advances*, 2015, **5**, 67267-67276.
88. A. George, K. Tran, T. J. Morgan, P. I. Benke, C. Berrueco, E. Lorente, B. C. Wu, J. D. Keasling, B. A. Simmons and B. M. Holmes, *Green chemistry*, 2011, **13**, 3375-3385.

Glycerol thermal processing  
200-240 °C

